Supporting information for "The Arctic has warmed four times faster than the globe since 1980"

Mika Rantanen[1,*], Alexey Karpechko[1], Antti Lipponen[1], Kalle Nordling[1], Otto Hyvärinen[1], Kimmo Ruosteenoja[1], Timo Vihma[1], and Ari Laaksonen[1]

[1]Finnish Meteorological Institute, Helsinki, Finland

[*]Correspondence to: mika.rantanen@fmi.fi

1 Observational data

Dataset	Abbreviation	Resolution	Period	Reference
ERA5 reanalysis	ERA5	0.25°	1950-2019	Hersbach et al. (2020)
NASA GISTEMP v4	GISTEMP	2°	1900-2019	Lenssen et al. (2019)
Berkeley Earth	BEST	5°	1900-2019	Rohde and Hausfather (2020)
Cowtan & Way v2.0	CW	5°	1900-2019	Cowtan and Way (2014)

Table S1: Observational datasets used in this study.

The three in-situ datasets (GISTEMP, BEST and CW) are merged land-ocean indices, i.e. they use station data on land areas and sea surface temperatures (SSTs) above the oceans. GISTEMP relies largely on Global Historical Climatology Network Monthly version 4 (Menne et al., 2018) on land surface. BEST has its own land surface record (Rohde et al., 2013a,b), and CW is based on the CRUTEM4 database (Jones et al., 2012). For SSTs, GISTEMP uses Extended Reconstruction Sea Surface Temperature version 5 of NOAA (Huang et al., 2015). BEST and CW use the HadSST3 dataset (Kennedy et al., 2011).

2 Climate models

Model ensemble	Forcing	Ensemble size	Period	Reference
CMIP5	RCP8.5	35	1850-2099	Taylor et al. (2012)
CMIP6	SSP2-4.5/SSP5-8.5	31/32	1850-2099	Eyring et al. (2016)
MPI-GE	RCP8.5	100	1850-2099	Maher et al. (2019)

Table S2: Climate model ensembles used in this study.

Model name	tas
ACCESS1-0	x
ACCESS1-3	x
BCC-CSM1-1	x
BCC-CSM1-1-M	x
BNU-ESM	x
CanESM2	x
CCSM4	x
CESM1-BGC	x
CESM1-CAM5	x
CMCC-CESM	x
CMCC-CM	x
CMCC-CMS	x
CNRM-CM5	x
CSIRO-Mk3-6-0	x
FGOALS-g2	x
FIO-ESM	x
GISS-E2-H	x
GISS-E2-H-CC	x
GISS-E2-R	x
GISS-E2-R-CC	x
HadGEM2-AO	x
HadGEM2-CC	x
HadGEM2-ES	x
INMCM4	x
IPSL-CM5A-LR	x
IPSL-CM5A-MR	x
IPSL-CM5B-LR	x
MIROC5	x
MIROC-ESM	x
MIROC-ESM-CHEM	x
MPI-ESM-MR	x
MRI-CGCM3	x
MRI-ESM1	x
MPI-ESM-LR	x
NorESM1-M	x

Table S3: CMIP5 models used in this study

Model name	tas	sic
ACCESS-CM2	x	x
ACCESS-ESM1-5	x	x
AWI-CM-1-1-MR	x	
BCC-CSM2-MR	x	x
CAMS-CSM1-0	x	x
CanESM5	x	
CESM2	x	x
CESM2-WACCM	x	x
CMCC-CM2-SR5	x	
CNRM-CM6-1	x	x
CNRM-ESM2-1	x	x
EC-Earth3	x	x
EC-Earth3-Veg	x	x
FGOALS-f3-L	x	x
FGOALS-g3	x	x
GFDL-ESM4	x	x
GISS-E2-1-G	x	
HadGEM3-GC31-LL	x	x
INM-CM4-8	x	x
INM-CM5-0	x	x
IPSL-CM6A-LR	x	
KACE-1-0-G	x	
MIROC6	x	x
MIROC-ES2L	x	x
MPI-ESM1-2-HR	x	x
MPI-ESM1-2-LR	x	x
MRI-ESM2-0	x	x
NESM3	x	x
NorESM2-LM	x	x
NorESM2-MM	x	x
TaiESM1	x	
UKESM1-0-LL	x	x

Table S4: CMIP6 models used in this study. Columns 2 and 3 indicate the availability of 2-meter temperature (tas) and sea-ice concentration (sic) data.

3 Supplementary figures

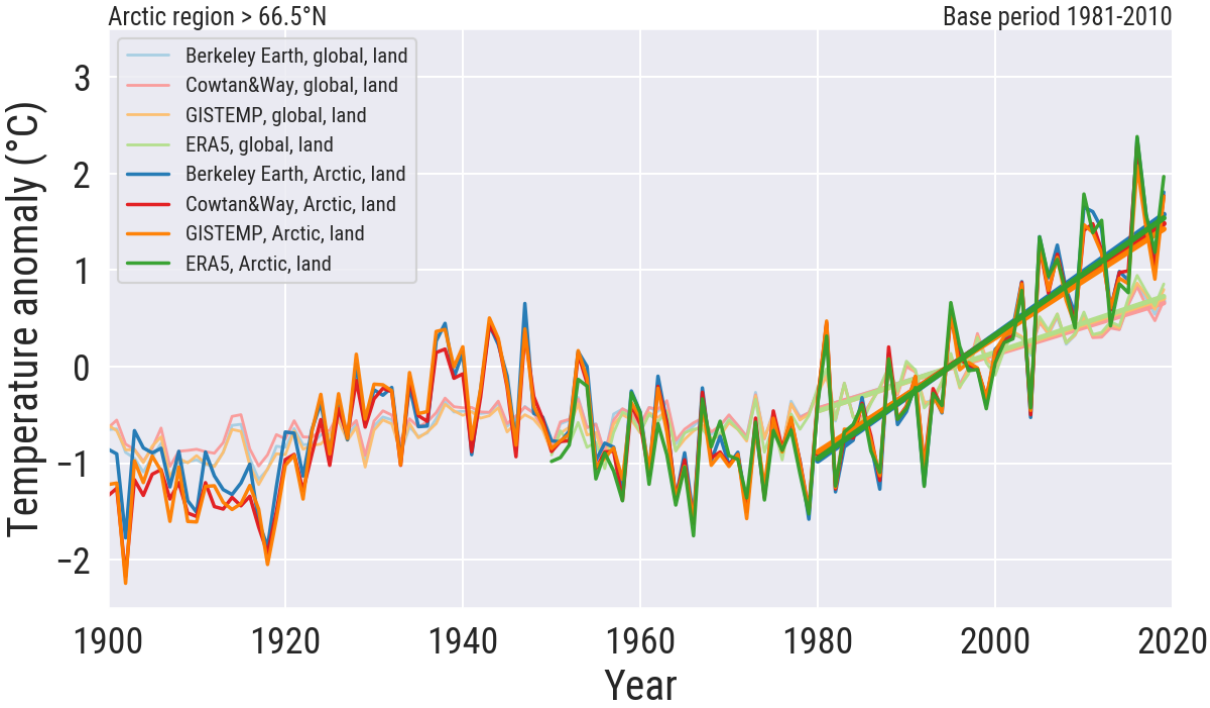

Figure S1: Annual mean temperature anomalies in the Arctic and global land areas during 1900-2019 derived from the various observational datasets (see the legend). Temperature anomalies have been calculated relative to the 1981-2010 period. Shown are also the linear temperature trends for 1980-2019.

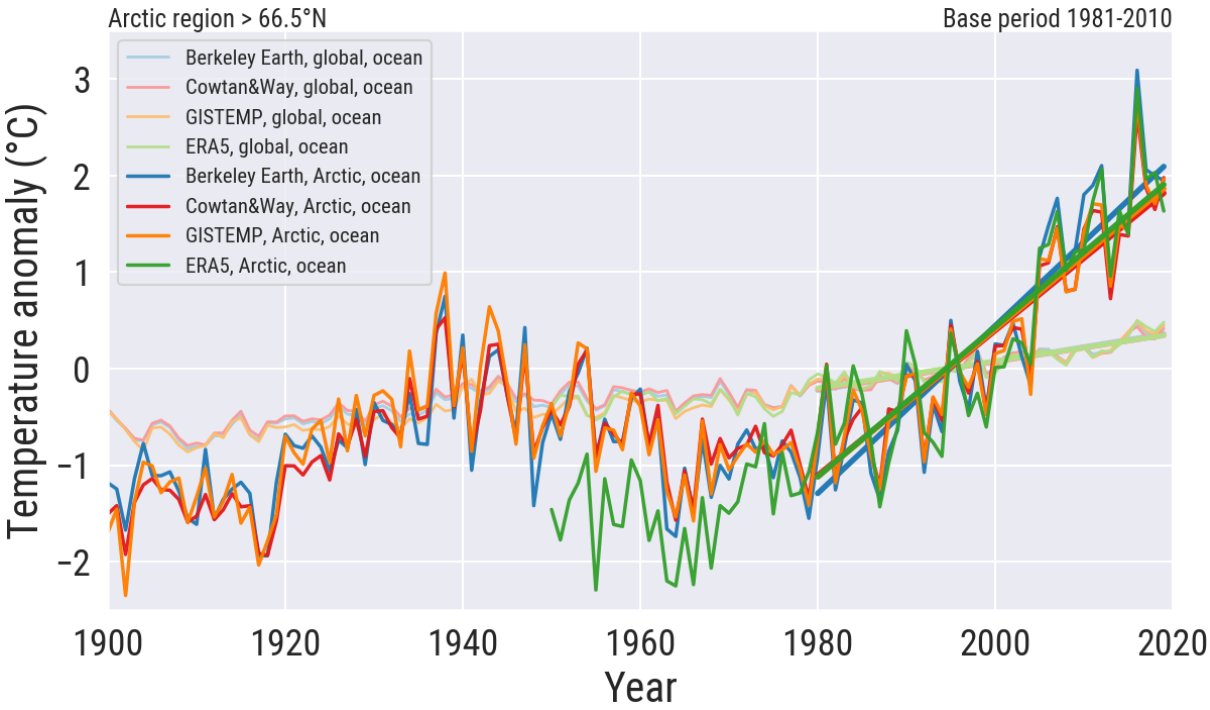

Figure S2: Same as Fig. S1 but for the ocean.

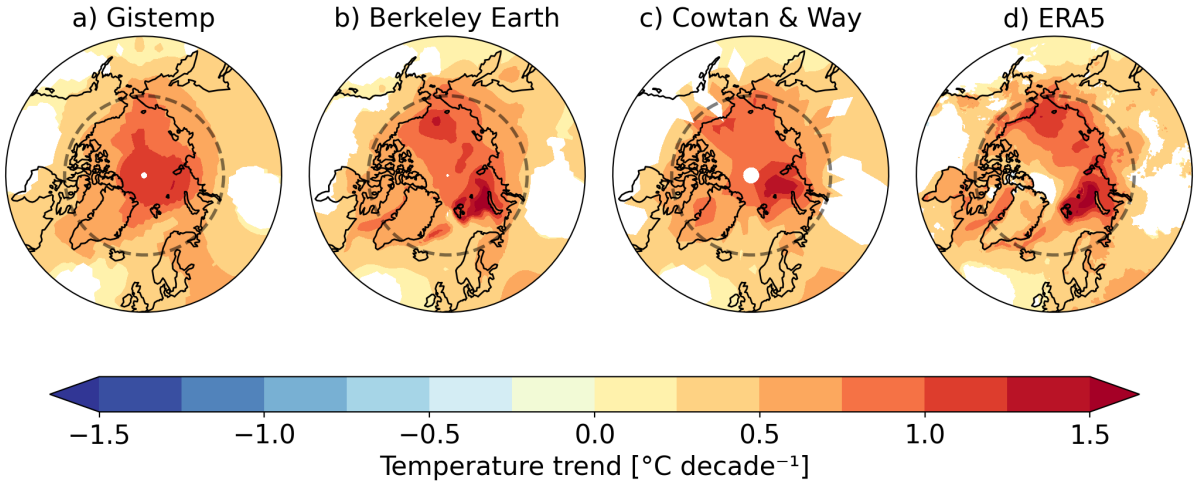

Figure S3: Annual mean temperature trends for the period 1980-2019 derived from a) NASA GISTEMP v4, b) Berkeley Earth, c) Cowtan & Way, and d) ERA5 reanalysis. Dashed line indicates the Arctic Circle (66.5°N latitude). Areas without a statistically significant change (determined using a two-sided Wald t-test, with $P < 0.05$ indicating a significant difference) are masked out.

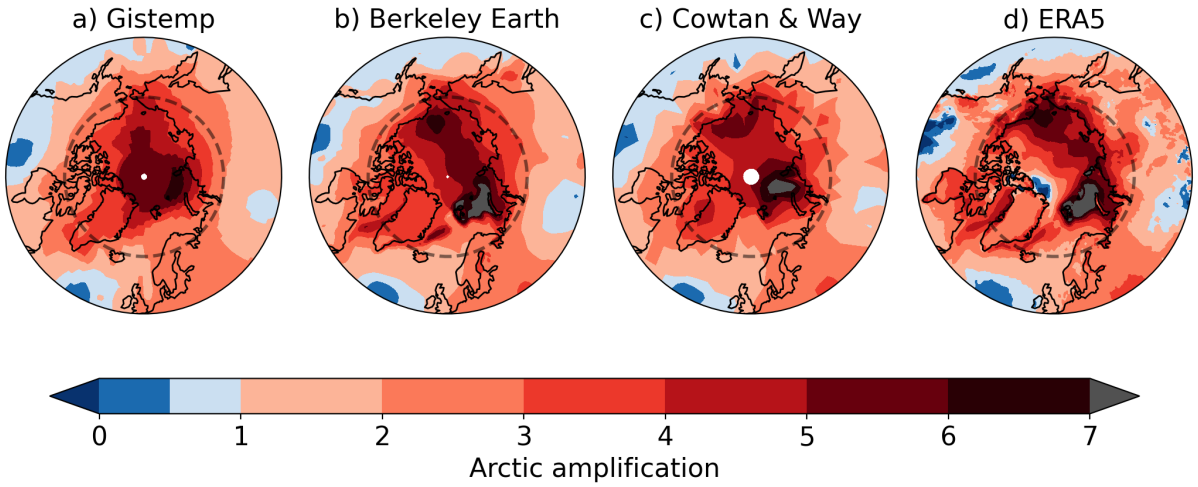

Figure S4: Arctic amplification for the period 1980-2019 derived from a) NASA GISTEMP v4, b) Berkeley Earth, c) Cowtan & Way, and d) ERA5 reanalysis. Dashed line indicates the Arctic Circle (66.5°N latitude).

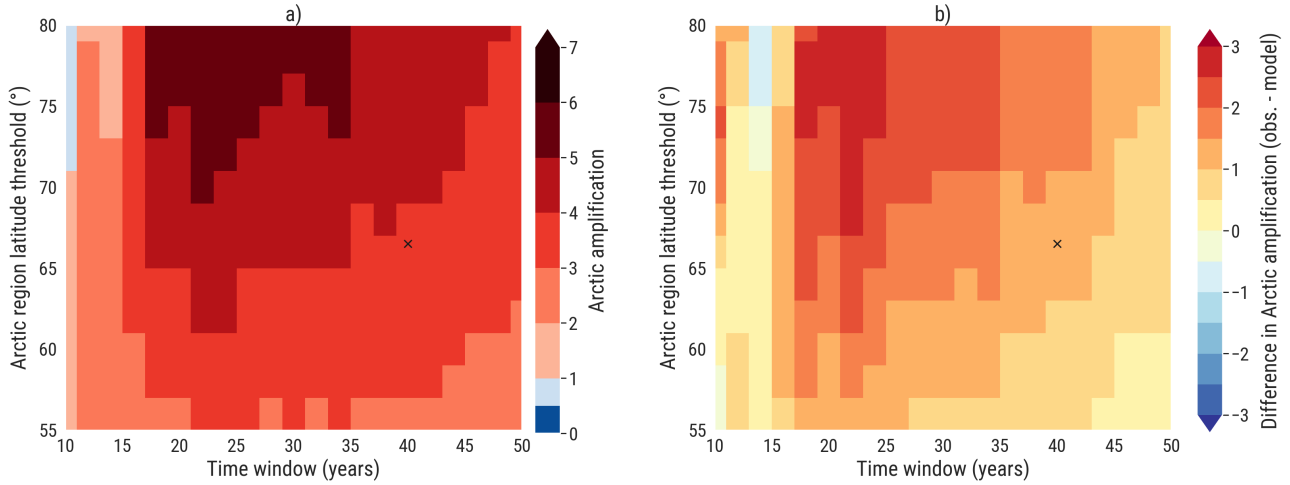

Figure S5: Sensitivity of AA (a) and the difference of AA between CMIP6 ensemble mean and observations (b) to the time window used in calculating the linear trends (x-axis) and the southern boundary of the Arctic (y-axis). The end year of all linear trends (x-axis) is 2019. The cross marks the baseline value used in the study, estimated with 40-year linear trends and the southern boundary of 66.5°N.

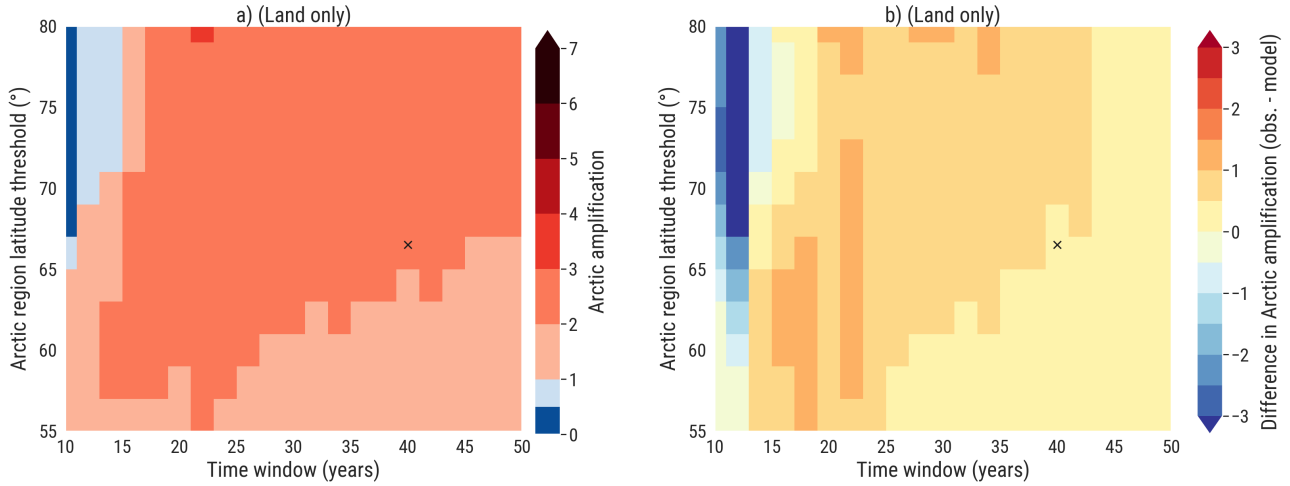

Figure S6: Same as Fig. S5 but for land areas only.

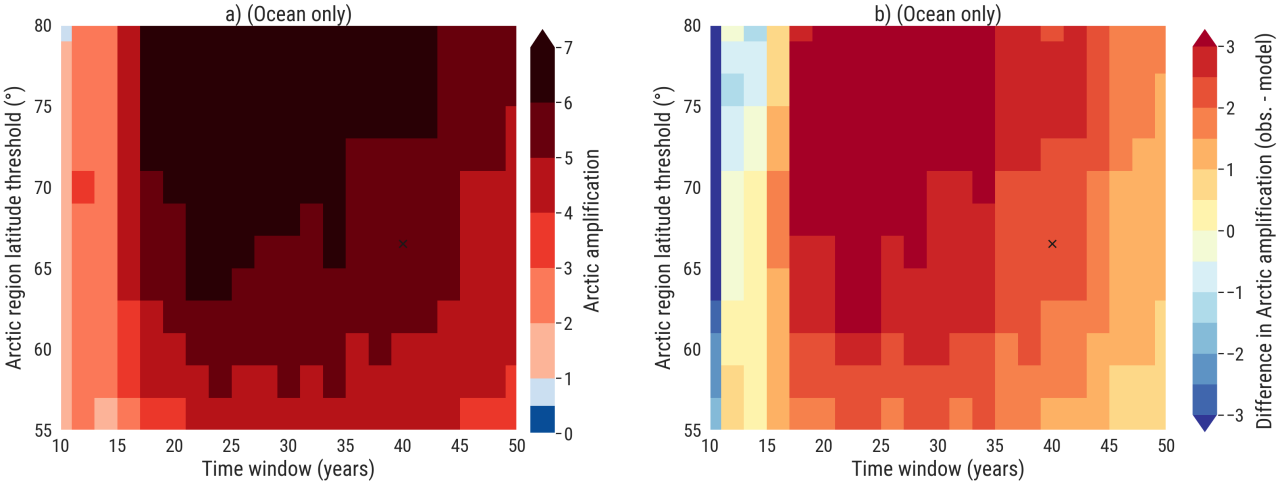

Figure S7: Same as Fig. S5 but for ocean only.

	Jan	Feb	Mar	Apr	May	Jun	Jul	Aug	Sep	Oct	Nov	Dec
ERA5 reanalysis	4.8	3.8	3.7	5.3	2.8	2.0	1.5	2.1	3.6	5.0	5.1	4.5
NASA GISTEMP v4	5.0	4.2	3.7	4.8	2.9	2.3	1.9	2.0	2.7	4.2	5.3	4.9
Berkeley Earth	5.6	4.8	4.0	5.0	3.0	2.2	1.9	2.1	3.2	5.3	6.0	5.2
Cowtan & Way	5.1	4.4	3.9	4.7	3.0	2.3	2.0	2.4	2.8	4.2	5.2	4.6
Average of the datasets	5.1	4.3	3.8	5.0	2.9	2.2	1.8	2.2	3.1	4.7	5.4	4.8

Figure S8: Arctic amplification in different months and in different obsevational datasets for 1980-2019 using Arctic area definition 66.5°-90°N. The bottom row shows the average of the four datasets.

References

Cowtan, K. and Way, R. G. (2014). Coverage bias in the HadCRUT4 temperature series and its impact on recent temperature trends. *Quarterly Journal of the Royal Meteorological Society*, 140(683):1935–1944.

Eyring, V., Bony, S., Meehl, G. A., Senior, C. A., Stevens, B., Stouffer, R. J., and Taylor, K. E. (2016). Overview of the Coupled Model Intercomparison Project Phase 6 (CMIP6) experimental design and organization. *Geoscientific Model Development*, 9(5):1937–1958.

Hersbach, H., Bell, B., Berrisford, P., Hirahara, S., Horányi, A., Muñoz-Sabater, J., Nicolas, J., Peubey, C., Radu, R., Schepers, D., et al. (2020). The ERA5 global reanalysis. *Quarterly Journal of the Royal Meteorological Society*.

Huang, B., Banzon, V. F., Freeman, E., Lawrimore, J., Liu, W., Peterson, T. C., Smith, T. M., Thorne, P. W., Woodruff, S. D., and Zhang, H.-M. (2015). Extended reconstructed sea surface temperature version 4 (ERSST. v4). Part I: Upgrades and intercomparisons. *Journal of climate*, 28(3):911–930.

Jones, P., Lister, D., Osborn, T., Harpham, C., Salmon, M., and Morice, C. (2012). Hemispheric and large-scale land-surface air temperature variations: An extensive revision and an update to 2010. *Journal of Geophysical Research: Atmospheres*, 117(D5).

Kennedy, J., Rayner, N., Smith, R., Parker, D., and Saunby, M. (2011). Reassessing biases and other uncertainties in sea surface temperature observations measured in situ since 1850: 1. measurement and sampling uncertainties. *Journal of Geophysical Research: Atmospheres*, 116(D14).

Lenssen, N. J., Schmidt, G. A., Hansen, J. E., Menne, M. J., Persin, A., Ruedy, R., and Zyss, D. (2019). Improvements in the GISTEMP uncertainty model. *Journal of Geophysical Research: Atmospheres*, 124(12):6307–6326.

41 Maher, N., Milinski, S., Suarez-Gutierrez, L., Botzet, M., Dobrynin, M., Kornblueh, L., Kröger,
42 J., Takano, Y., Ghosh, R., Hedemann, C., et al. (2019). The Max Planck Institute Grand
43 Ensemble: enabling the exploration of climate system variability. *Journal of Advances in*
44 *Modeling Earth Systems*, 11(7):2050–2069.

45 Menne, M. J., Williams, C. N., Gleason, B. E., Rennie, J. J., and Lawrimore, J. H. (2018).
46 The global historical climatology network monthly temperature dataset, version 4. *Journal*
47 *of Climate*, 31(24):9835–9854.

48 Rohde, R., Muller, R., Jacobsen, R., Muller, E., Perlmutter, S., Rosenfeld, A., Wurtele, J.,
49 Groom, D., and Wickham, C. (2013a). A New Estimate of the Average Earth Surface Land
50 Temperature Spanning 1753 to 2011. *Geoinformatics & Geostatistics: An Overview*, 7:2.

51 Rohde, R., Muller, R., Jacobsen, R., Perlmutter, S., Rosenfeld, A., Wurtele, J., Curry, J.,
52 Wickhams, C., and Mosher, S. (2013b). Berkeley Earth Temperature Averaging process.
53 *Geoinformatics & Geostatistics: An Overview*, 1(2):20–100.

54 Rohde, R. A. and Hausfather, Z. (2020). The Berkeley Earth land/ocean temperature record.
55 *Earth System Science Data*, 12(4):3469–3479.

56 Taylor, K. E., Stouffer, R. J., and Meehl, G. A. (2012). An overview of CMIP5 and the
57 experiment design. *Bulletin of the American Meteorological Society*, 93(4):485–498.